A low-transition-temperature electrolyte based on ethylene glycol for rechargeable zinc-ion batteries

Electrochimica Acta 525 (2025) 146061

Contents lists available at ScienceDirect

Electrochimica Acta

journal homepage: www.journals.elsevier.com/electrochimica-acta

A low-transition-temperature electrolyte based on ethylene glycol for rechargeable zinc-ion batteries

Matteo Palluzzi [a], Marita Afiandika [b,c], Shizhao Xiong [b], Akiko Tsurumaki [a,d], Paola D'Angelo [a], Aleksandar Matic [b,c], Maria Assunta Navarra [a,d,*]

[a] Department of Chemistry, Sapienza University of Rome, P.le A. Moro 5, 00185, Rome, Italy
[b] Department of Physics, Chalmers University of Technology, 41296, Göteborg, Sweden
[c] Wallenberg Wood Science Centre, Chalmers University of Technology, Gothenburg, 41296, Sweden
[d] Hydro-Eco Research Center, Sapienza University of Rome, Via A. Scarpa 16, 00161, Rome, Italy

ARTICLE INFO

Keywords:
low-transition-temperature mixtures
electrolytes
zinc-ion batteries

ABSTRACT

Zinc-ion batteries (ZIBs) offer promising energy storage solutions due to their high capacity, abundance and low cost of raw materials, and stability in air of zinc. Despite these advantages, ZIBs with aqueous electrolytes struggle with issues like dendrite formation, hydrogen evolution, and zinc corrosion. This study explores the use of low-transition-temperature (LTT) mixtures as electrolytes to address these critical issues of ZIBs. Novel LTT electrolytes at different molar ratios of $Zn(TFSI)_2$ and ethylene glycol (EG), chosen for their cost-effectiveness, were prepared. The LTT electrolytes were characterized, through spectroscopic and electrochemical methods, and the most promising one (Zn:EG 1:7) was further evaluated in a full cell by coupling Zn metal with a K^+-doped vanadium oxide ($K_{0.5}V_2O_5$, KVO) cathode. The full cell shows an excellent stability upon cycling and notable suppression of the dendritic growth, but limited capacities. Our electrolyte system holds significant potential for advancing ZIB technology if further developed.

1. Introduction

The demand for energy stands out as one of the primary challenges facing society today. Beyond the imperative to develop reliable and sustainable electricity production methods, it is crucial to address the efficient storage of energy and its utilization as needed. Rechargeable batteries, particularly lithium-ion batteries (LIBs), serve as the cornerstone technology for this purpose, but they still face several shortcomings: significant safety issues, the need of substantial investments to handle lithium, and the need for critical raw materials, such as cobalt, graphite and lithium itself[1].

Considering these factors, alternative chemistries based on multivalent ions (Mg^{2+}, Zn^{2+}, Al^{3+}) have been proposed[2]. Zn-ion batteries (ZIBs), in particular, are appealing due to the high volumetric (5851 mAh/cm^3) and gravimetric (820 mAh/g) capacity of zinc metal as anode, its abundance (constituting 75 ppm of Earth's crust), low cost of extraction[1], widespread distribution on Earth[1], stability in air (allowing for processing and production without the need of a controlled atmosphere), and compatibility with aqueous electrolytes (which significantly enhances device safety). However, the commercialization of ZIBs employing aqueous electrolytes is still hindered by several issues: dendrite formation leading to rapid device failure, hydrogen evolution from electrochemical water splitting, and corrosion and passivation of zinc due to side reactions with water[3].

To mitigate hydrogen evolution and side reactions, the replacement of aqueous electrolytes with low-transition-temperature (LTT) mixtures, which do not compromise the safety of the device due to their low volatility and flammability, has been proposed[3–5]. Furthermore, the use of LTT mixtures is appealing for their simple preparation and eco-friendliness[5,6]. In the literature, it is quite common to use the terms "eutectic" or even "deep eutectic solvents" to refer generally to any systems in which the mixture of two components has a lower melting temperature than the individual components[7–11]. However, the term eutectic should specifically denote the mixture of two components with the lowest possible melting temperature[12]. Furthermore, due to the complex kinetic behavior of these mixtures, it is often difficult to observe

In memory of Professor Bruno Scrosati (August 1937 – November 2024), a mentor leading the research in the battery field worldwide.

* Corresponding author.
E-mail address: mariassunta.navarra@uniroma.it (M.A. Navarra).

https://doi.org/10.1016/j.electacta.2025.146061
Received 18 November 2024; Received in revised form 12 February 2025; Accepted 15 March 2025
Available online 20 March 2025

their crystallization and accurately assess their melting temperature, making the classification of eutectic or deep eutectic solvents even more challenging[7,8,10]. For these reasons, we prefer the broader term LTT mixtures to refer to our systems[12].

To address the dendrite growth on zinc metal anodes, the formation of a stable anion-based solid electrolyte interphase (SEI), by using fluorine-containing salts (such as zinc(II) bis(trifluoromethanesulfonyl) imide, $Zn(TFSI)_2$), has been suggested as an effective strategy[7]. The key to form this anion-based SEI lies in controlling the Zn solvation structure in the electrolyte in order to obtain anion-containing Zn solvates[4]. LTT electrolytes provide a facile route to achieve this by the simple regulation of the molar ratios of electrolyte components, with the added benefits of low cost, environmental friendliness, and straightforward preparation[5,13]. All these benefits make LTT mixtures extremely attractive as electrolytes for ZIBs.

In this study, we prepared a novel LTT mixture based on $Zn(TFSI)_2$ and ethylene glycol (EG) and explored its potential as an electrolyte for ZIBs. $Zn(TFSI)_2$ was selected for the beneficial effects of the $TFSI^-$ anion on the formation of a F-rich SEI[7], while EG was selected for its affordability to balance the cost of the zinc salt. Mixtures at various molar ratios were prepared and characterized using a spectroscopic and electrochemical techniques, the former to gain knowledge on the rearrangement of the molecules in the mixtures, and the latter to evaluate their performance as electrolytes. The most promising mixture for battery applications (Zn:EG 1:7) was then tested as an electrolyte in a full cell with a Zn metal anode, a novel K^+-doped vanadium oxide ($K_{0.5}V_2O_5$, KVO)[14] cathode material, demonstrating encouraging results for ZIB.

2. Experimental

2.1. LTT electrolyte preparation

EG (anhydrous, 99.8%) was purchased from Merck KGaA (Darmstadt, Germany), while $Zn(TFSI)_2$, (99.5%) was obtained from Solvionic and stored in an Ar-filled glove box. Nine mixtures of the two reagents were prepared, with molar ratios of EG:Zn of 2, 4, 6, 7, 8, 9, 10, 12, and 20. To ensure the correct molar ratio, the appropriate amount of Zn $(TFSI)_2$ was weighed inside the glove box, transferred outside, and then the desired amount of EG was added. The mixtures were then heated up to 80°C and stirred for 2 hours. Homogeneous, colorless, and quite viscous solutions (with viscosity decreasing with a higher amount of EG) were obtained for the molar ratios of 6, 7, 8, 9, 10, 12, and 20 (EG/Zn), while undissolved salt was observed for higher Zn-salt concentrations (molar rations ratios of 2 and 4). Consequently, these two mixtures were discarded from further experiments. Tab. 1 shows the molar ratios, the molar fractions, and the molality of the mixtures.

2.2. Characterization of the LTT electrolytes

Differential scanning calorimetry (DSC) was performed using a DSC250 from TA Instruments, with a heating rate of 5°C/min between -100 and 100°C, using an empty pan as a reference. ATR-FTIR analyses were conducted in an Ar-filled glove box using a Bruker Alpha FTIR spectrometer equipped with a diamond crystal. The procedure consisted of 240 scans for the background and 240 scans for the sample, with a resolution of 2 cm^{-1}. Raman data were recorded using a Bruker MultiRAM FT-Raman spectrometer with a spectral resolution of 2 cm^{-1}, using a Nd laser (1064 nm, 300 mW) as the excitation source and averaged over 4000 scans. The ionic conductivities were determined using an AMEL 160 conductivity meter. A suitable amount of electrolyte was placed in a sealed glass conductivity cell (AMEL 192/K1) equipped with two porous platinum electrodes (cell constant: 0.987 cm^{-1}). All operations were carried out inside an Ar-filled glove box. Conductivity measurements were performed over a temperature range of −40°C to 80°C using a climatic test chamber (Binder GmbH MK53).

To ensure crystallization, the cell was briefly immersed in liquid nitrogen before being transferred to the climatic chamber at −40°C. After a few minutes at this temperature, the solidified sample reverted to its liquid state. This process was repeated multiple times, consistently confirming a melting point below −40°C. Following overnight storage at −40°C, a controlled heating scan was conducted: initially at 1°C/h up to 20°C, then at 2°C/h up to 80°C. Conductivity measurements were recorded at 5°C intervals throughout the process.

Table 1
Molar ratios, molar fractions ($\chi_{(Zn\ salt)}$) and concentration (Conc. (m)) of the zinc salt (expressed as molality) of the seven successfully prepared LTT electrolytes.

Zn/EG molar ratio	1:6	1:7	1:8	1:9	1:10	1:12	1:20
$\chi_{(Zn\ salt)}$	0.143	0.125	0.111	0.100	0.091	0.077	0.048
Conc. (m)	2.69	2.30	2.01	1.79	1.61	1.34	0.81

2.3. Preparation of the KVO electrode

The synthesis procedure of KVO has previously been reported in Ref. [14]. The KVO was mixed with conductive carbon and poly(vinylidene fluoride) in a weight ratio of 70:20:10 and pressed with a force of 3 tons to produce self-standing electrodes with a diameter of 13 mm and a weight between 20 and 30 mg.

2.3. Preparation of the cells and electrochemical tests

For all electrochemical tests, CR2032 coin cells were assembled outside the glove box. A single Whatman glass fiber separator (GF/C) soaked in 60 μL of electrolyte (either a LTT mixture or a 2 M solution of $ZnSO_4$ in water used as a reference) was employed for all the cells. For the stripping/plating tests and impedance spectroscopy analysis, symmetric Zn||Zn cells (electrodes obtained from foils purchased from Goodfellow, with a diameter of 14 mm and a thickness of 100 μm) were used. For the coulombic efficiency evaluation and galvanostatic cycling, a zinc electrode was coupled with a copper working electrode in the former case, or a KVO cathode in the latter. After the assembly of the Zn||Zn and Zn||Cu cells, a resting period of 1 hour was applied before electrochemical tests, while for the Zn||KVO cells, a 4-hour resting period was applied.

Galvanostatic stripping/plating tests were performed at current density of 0.1 mA/cm^2, a capacity of 0.1 mAh/cm^2, and a cut-off potential of ±1.2 V (vs. Zn^{2+}/Zn). To evaluate the electrolyte resistances, identical cells were assembled and subjected to the same procedure for 10 cycles, recording electrochemical impedance spectroscopy (EIS) between 0.1 Hz and 100 kHz before and after each cycle.

To evaluate the coulombic efficiencies, a novel procedure proposed by Adams *et al.*[15] was followed. The procedure consists of an extended plating on Cu at 0.1 mA/cm^2 for 10 hours, followed by an extended stripping at the same current density until a potential of 0.5 V (vs Zn^{2+}/Zn) was reached. After that, a second long plating at 0.1 mA/cm^2 for other 10 hours was performed (the obtained capacity is denoted Q_T), followed by ten cycles of charge/discharge at the same current density, each with a duration of 1 hour (the capacity of each of these cycles is denoted Q_C). Lastly, a final stripping at 0.1 mA/cm^2 was performed until a cut-off potential of 0.5 V (vs. Zn^{2+}/Zn) was reached (the obtained capacity is denoted Q_S). The final coulombic efficiency obtained by this procedure is calculated from:

$$CE = \frac{10Q_C + Q_S}{10Q_C + Q_T}$$

To evaluate the electrochemical stability window of the electrolyte (ESW), two Zn||C coin-cells were assembled. The two cells were tested at a scan rate of 0.2 mV/s, with the potential range extended up to 2.5 V vs Zn^{2+}/Zn and -0.5 V vs Zn^{2+}/Zn, respectively. The working electrodes were prepared by producing a slurry with N-methylpyrrolidone (NMP)

as the solvent, in which conductive carbon (Super-P, Timcal, Bodio, Switzerland) and poly(vinylidene fluoride) (PVDF 6020, Solvay, Brussels, Belgium) were dispersed in a weight ratio of 70:30. This slurry was applied onto an aluminum foil current collector using the doctor blade technique. After the NMP was removed, the electrodes were punched into 1 cm diameter disks and dried overnight at 100°C under vacuum.

Lastly, the LTT electrolytes were tested as electrolytes in Zn||KVO cells by galvanostatic cycling with a current of 10 mAh/g (calculated with respect to the mass of the active material) and imposing 1.4 V and -0.4 V as cut-off potentials. All the electrochemical tests, with the exception of the EIS and ESW measurements, were performed using a Scribner 580 Battery Test System, while EIS and ESW measurements were recorded using a Bio-Logic VMP-3 potentiostat.

2.4. Post-mortem characterization of the electrodes

The zinc electrodes retrieved from the Zn||KVO cells were washed with water and dried, then subsequently treated with an ultrasonic bath at 60 kHz for 15 minutes in water, followed by a second drying step. Scanning electron microscopy (SEM) was performed using a Phenom ProX (Thermo Fisher) to analyze the electrode morphology, while energy-dispersive spectroscopy (EDS) was conducted with the same instrument to determine their chemical composition. The analyses were performed using a beam-voltage of 15 kV.

3. Results and discussion

3.1. Characterization of the LTT electrolytes

The thermal behavior of the LTT electrolytes was evaluated through DSC and compared with the single components. Fig. 1 shows the DSC traces from the electrolytes, while the traces corresponding to the individual components are reported in **Fig. S1**. As it can be seen, the addition of zinc salt to EG completely suppress the tendency for crystallization at sub-zero temperatures, leaving only a glass transition (T_g) well below -70°C. The absence of the melting point of EG (expected at -13°C) confirms the lack of any isolated EG cluster, demonstrating the realization of a homogenous solution[10]. Interestingly, the less zinc salt is added, the more T_g shifts to lower temperatures, not being observed even at -100°C in the case of a Zn:EG 1:20 molar ratio. Furthermore, no other transitions are observed up to 100°C, confirming the extreme compatibility of these mixtures with battery applications. The absence of an observed melting point makes it impossible to formally define the mixtures as eutectics and confirming that the term "low--transition-temperature mixtures" is more appropriate[12]. However, it should be noted that a similar behaviour has been observed in many other eutectic mixtures and even in deep eutectic solvents due to their complex kinetics of their transitions[7,8,10], so the absence of an observed melting point can be ascribed to this phenomena too.

To confirm the formation of an H-bonds network, ATR-FTIR and Raman spectroscopy were performed. The spectra obtained from ATR-FTIR are shown in Fig. 2. The mixing of the two components (Zn $(TFSI)_2$ and EG) results in interactions, as evidenced by the fact that the spectra of the mixtures are not simply the sum of the spectra of the individual components (see Fig. 2**a**). For example, the peak at 1147 cm^{-1}, corresponding to the stretching of the S-O bond in $TFSI^-$, is red-shifted upon the addition of EG. This effect is even more evident in Fig. 2**b**, which highlights a progressive reduction in the intensity of the peak centered at 3300 cm^{-1} in EG and the appearance of a shoulder at approx. 3500 cm^{-1}, both related to O-H stretching and thus sensitive to hydrogen bonding, upon the progressive addition of the salt. These changes indicate the formation of new coordination types involving the O-H groups. Additionally, the bands corresponding to the symmetric and asymmetric stretching of C-H (at 2873 cm^{-1} and 2936 cm^{-1} in the case of EG) are blue-shifted upon the addition of the zinc salt. Since these groups are improper hydrogen bond-forming groups (groups where the H atom is not directly bonded to an extremely electronegative atom[16]), the blue-shift indicates the formation of stronger hydrogen bond interactions in the mixture of EG and the zinc salt as compared to pure EG [10].

The blue-shift of the C-H is also evident in the Raman spectra shown in Fig. 3**b**. These observations confirm that the addition of zinc salt significantly alters the hydrogen bond network of EG, weakening the original bonds and forming new ones between EG and the salt. Additionally, the peak at 860 cm^{-1} is associated with the different conformations of the O-C-C-O backbone of EG[17,18]. It is possible to infer that the changes in the shape of this peak, observed with varying relative amounts of the components, are related to conformational changes in EG induced by the presence of the zinc salt, further supporting the idea of interactions between the two.

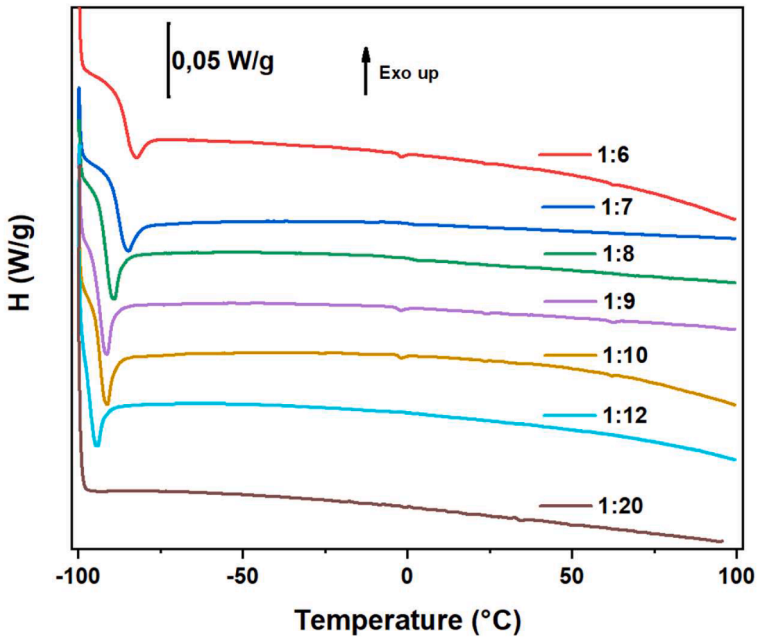

Figure 1. DSC traces of the LTT electrolytes at 6 different molar ratios (Zn/ EG).

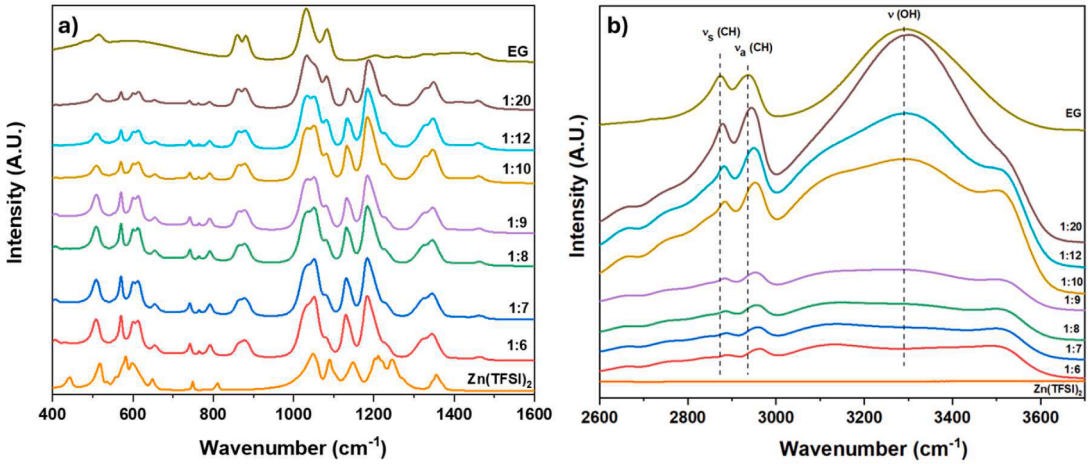

Figure 2. a) ATR-FTIR spectra of the six mixtures, EG and $Zn(TFSI)_2$ in the region between 400 and 1600 cm^{-1}. b) Zoom of the region between 2600 and 3700 cm^{-1} of the spectra.

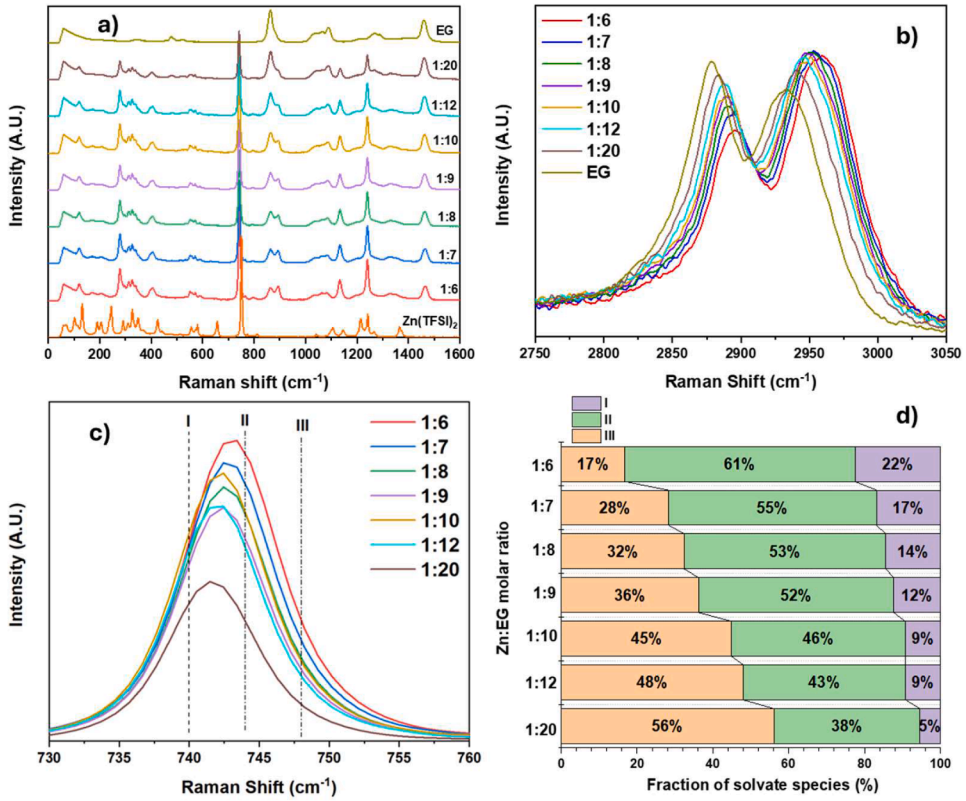

Figure 3. a) Raman spectra of the six mixtures, EG and $Zn(TFSI)_2$ in the region between 400 and 1600 cm^{-1}. b) Zoom of the region between 2750 and 3050 cm^{-1} of the spectra. c) Zoom of the region between 730 and 760 cm^{-1} of the spectra. The dotted lines denote the theoretical positions of the free TFSI anions in C_1 (I) and C_2 (II) conformations and TFSI anions coordinated to Zn-ions (III). d) Estimated solvate species distribution calculated from the Raman spectra.

To better analyze the association between Zn^{2+}, TFSI, and EG in the electrolytes, the region between 730 and 760 cm^{-1} was examined in detail. In this region it is possible to find the peak corresponding to the expansion and contraction of the whole TFSI anion, which is sensitive to changes in the environment surrounding the anion as well as its conformational state[19]. As shown in Fig. 3**c**, with increased EG concentration in the LTT electrolyte the peak shifts to lower wavenumbers. The peak has been deconvoluted into three components: one at 740 cm^{-1} (I), one at 744 cm^{-1} (II), and one at 751 cm^{-1} (III). I and II are assigned to free $TFSI^-$ in the two configuration C_1 and C_2, while III is assigned to the anions coordinated to Zn^{2+} [19]. The results of the analysis, with the distribution of the solvated species, is reported in Fig. 3**d**. As can be seen, up to an EG:Zn molar ratio of 9, more than 10% of anions are present in the solvation shell of Zn^{2+}. This is important for the formation of a stable anion-based SEI at the zinc electrode[4,7]. Considering this, the electrolytes with an EG/Zn molar ratio of 6 - 9 were considered for further electrochemical testing.

3.2. *Electrochemical tests*

One of the most critical parameters for zinc-ion batteries is the reversibility of the plating and stripping of zinc, which should occur

without side-reactions. To evaluate this, the four selected electrolytes were assessed in Zn||Cu using a novel coulombic efficiency[15] evaluation method cells as explained in the experimental section. The mixture with a molar ratio of 1:6 proved to be unsuitable as it was unable to sustain a current of 0.1 mA/cm^2 even for a few seconds without suffering from polarization, likely induced by the high viscosity. The results obtained for the other electrolytes are reported in Fig. 4**a, 4c, and 4e**. As can be seen, the electrolyte with a Zn:EG ratio of 1:7 provided the highest coulombic efficiency, reaching an average value of 95.85%.

Zn||Zn cells were also assembled to evaluate the bulk electrolyte resistances and their evolution over 10 cycles of stripping and plating at 0.1 mA/cm^2 (0.1 mAh/cm^2). As shown in Fig. 4**b, 4d, and 4f**, the bulk resistance for the electrolytes with Zn:EG ratio 1:7 and 1:8 is around 30 Ω, while for the 1:9 ratio it is around 20 Ω, likely due to the lower viscosity induced by the lower salt concentration. In all cases, the resistances appear to be extremely stable upon cycling.

Furthermore, the temperature dependence of the ionic conductivity of the electrolyte with a 1:7 Zn/EG ratio was investigated over a wide temperature range, from -40°C to 80°C. The results are reported in a conductivity plot in Fig. 5. This investigation clearly reveals that the mixture has a non-Arrhenius behavior, as previously reported in the literature for various DESs[20], i.e., a VTF trend, typical of amorphous electrolytes[21], was observed. The continuous increase in conductivity with temperature, without any sudden deflection, confirms that the LTT mixture melts at a temperature lower than -40°C. This finding, which aligns with the DSC data, demonstrates that even when using different experimental setups with significantly longer time scales, the thermal behavior of the mixture remains unchanged. Additionally, at 30°C, a satisfying ionic conductivity of 0.88 mS/cm was measured, further validating the promising properties of the selected electrolyte.

Due to all these favorable properties, this electrolyte composition has been selected for prolonged plating/stripping tests in Zn||Zn cells. The cell was cycled at a current density of 0.1 mA/cm^2 (capacity was 0.1 mAh/cm^2) and compared with an identical cell employing a 2 M solution of $ZnSO_4$ in water as a reference electrolyte. The results are reported in Fig. 6. As shown, the LTT electrolyte, while suffering from higher

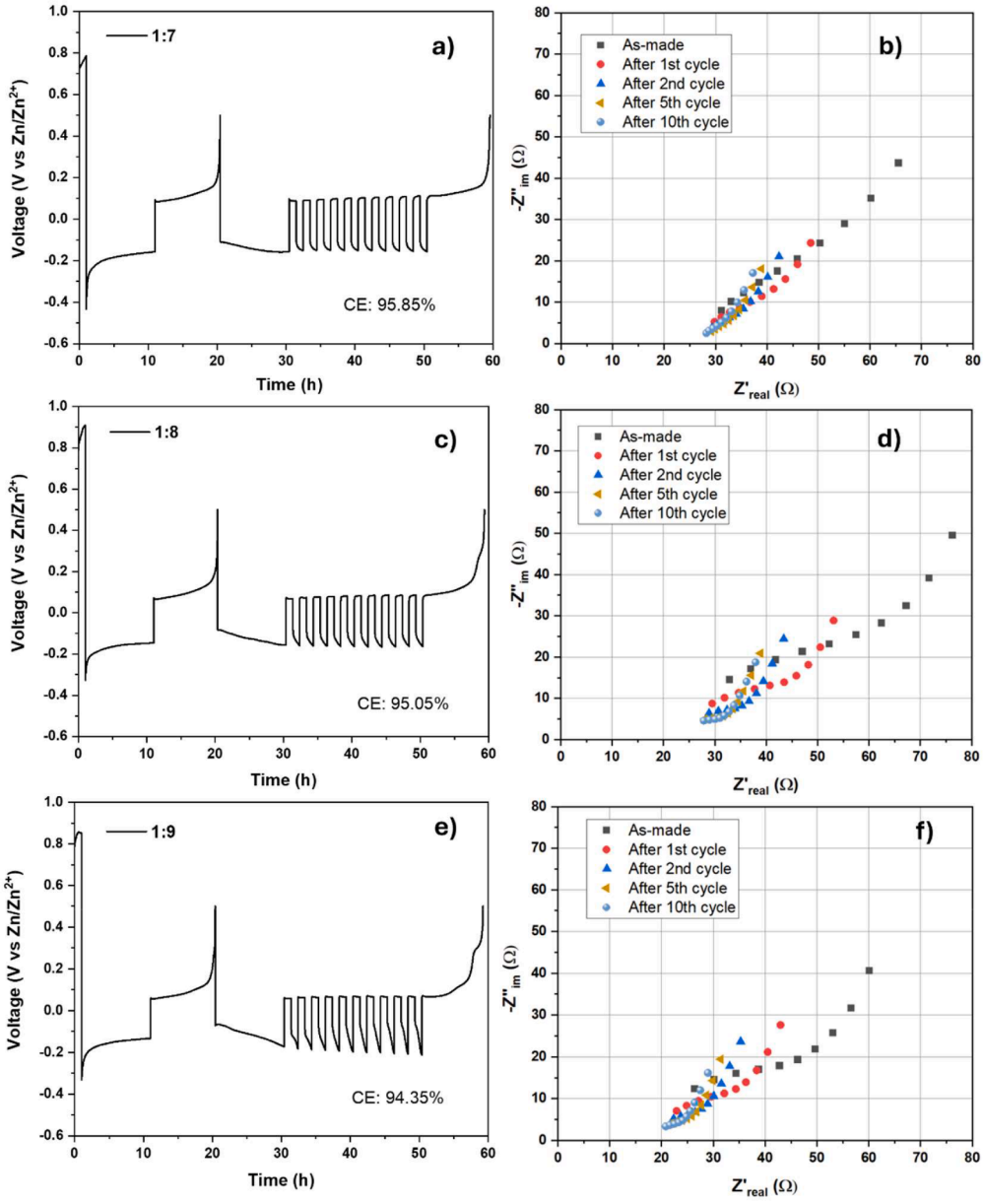

Figure 4. Voltage profiles obtained during the coulombic efficiency evaluation tests form cell using as electrolytes with Zn/EG ratios a) 1:7, c) 1:8, e) 1:9. High frequency region (3 - 100 kHz) of the electrochemical impedance spectra obtained from cells using electrolytes with Zn/EG ratios b) 1:7, d) 1:8, f) 1:9.

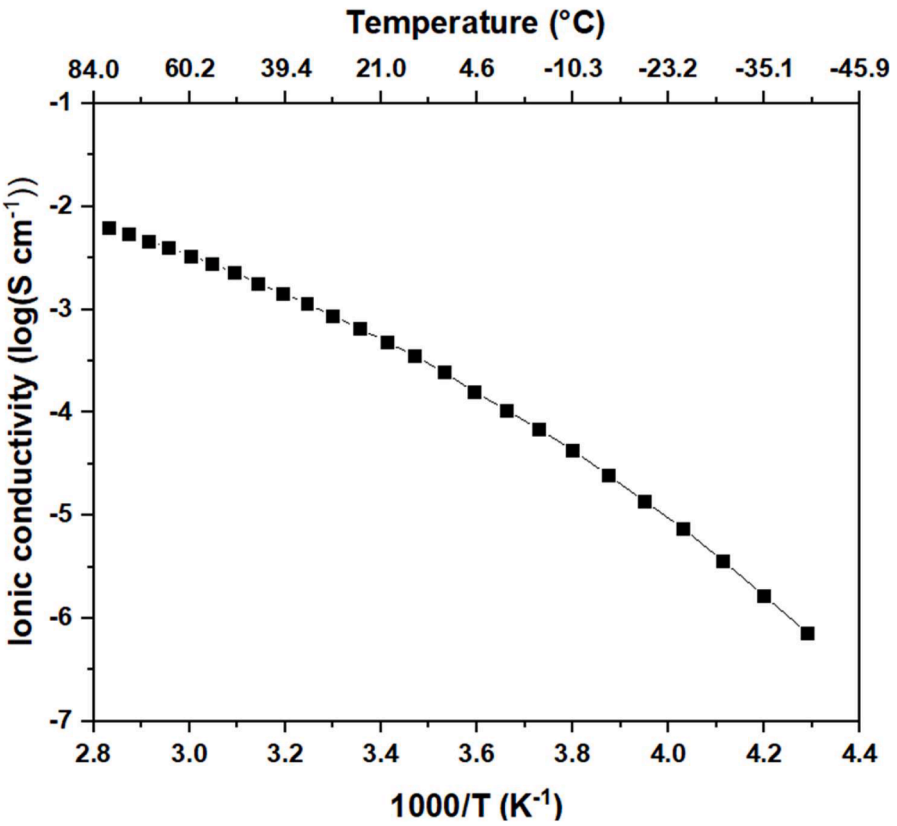

Figure 5. Conductivity plot of the 1:7 Zn/EG mixture.

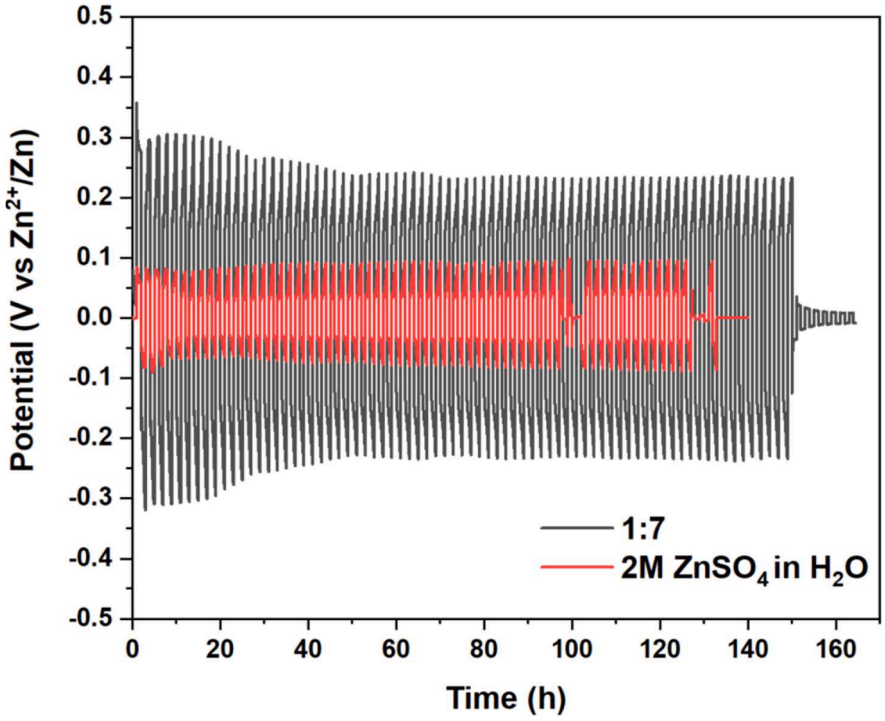

Figure 6. Stripping/plating test of the electrolyte with Zn/EG ratio 1:7 (in grey) compared to a 2M solution of $ZnSO_4$ in water as reference electrolyte (in red).

overpotential due to its viscosity and lower conductivity, was able to sustain the stripping/plating for around 150 hours before encountering a "*soft-short*"[22], surpassing the performance of the reference cell, which was able to sustain the plating/stripping for only around 100 hours before failure.

To evaluate the electrochemical stability window of the electrolyte, linear sweep voltammetry test was carried out in Zn||C cells (Fig. 7). The results show that the electrochemical stability window is around 2.73 V,

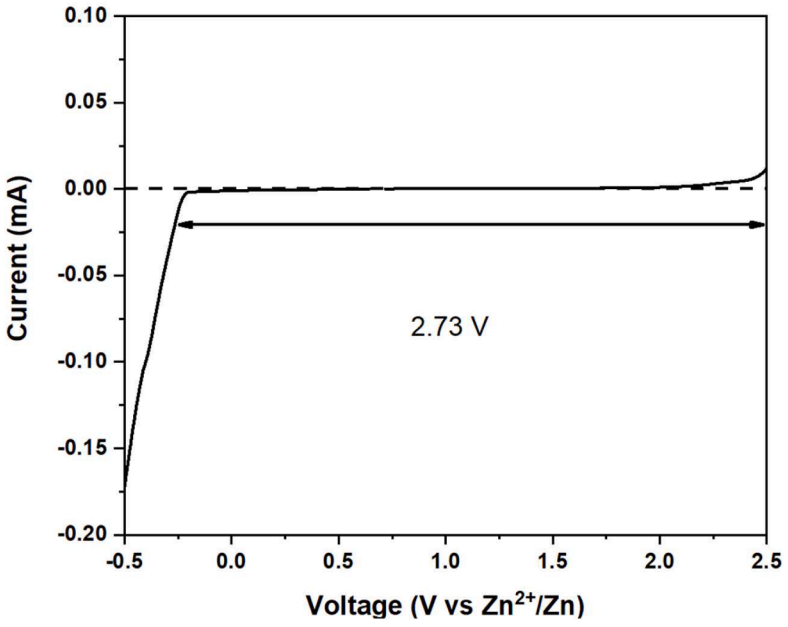

Figure 7. Linear sweep voltammetry of the electrolyte with a 1:7 Zn/EG ratio a Zn||C cells at a scan rate of 0.2 mV/s.

highlighting a notable stability of the electrolyte against both the H_2 and O_2 evolution.

Lastly, the selected electrolyte was tested in conjunction with a new cathode material, potassium-doped vanadium oxide[14]. Fig. 8 shows the voltage profiles obtained from the assembled cell. The cell was able to sustain 50 cycles of continuous intercalation/deintercalation at a current density of 10 mA/g (0.15 - 0.23 mA/cm^2), which is a notable result. However, the specific capacities of the cell are relatively low, with a maximum of 90 mAh/g in the 1st cycle, dropping to 50 mAh/g after 50 cycles. We attribute this to the rapid polarization encountered by the cell due to the high viscosity of the electrolyte.

Finally, to assess the effect of the electrolyte on zinc dendrite growth, Zn electrodes from Zn||KVO cells employing either the 1:7 LTT electrolyte or a 2 M solution of $ZnSO_4$ in water as electrolytes were retrieved after 10 cycles. Fig. 9 shows scanning electron microscopy (SEM) the images of the surface of the retrieved (after undergoing a thorough cleaning procedure) and pristine electrodes, highlighting that, in the case of the aqueous electrolyte, dendritic growth is extremely pronounced, with the typical hexagonal shape of zinc dendrites on the of Zn metal surface[23]. In contrast, no trace of dendritic growth was observed in the case of the LTT electrolyte, showing a surface more uniform and similar to the pristine one. The results of the EDS analysis are reported in **Tab. S1**. Notably, in the presence of the LTT electrolyte, a significantly higher carbon content was observed compared to the electrode cycled in 2 M $ZnSO_4$, where the detected carbon is attributed to the underlying carbon tape. This, combined with the presence of fluorine suggests that electrolyte components contributed to the formation of a passivation layer on the zinc electrode surface. We infer that this layer possesses protective properties for the zinc electrode and plays a crucial role in suppressing dendritic growth in the LTT electrolyte system. The traces of vanadium detected in both cases are likely due to detached cathode material particles.

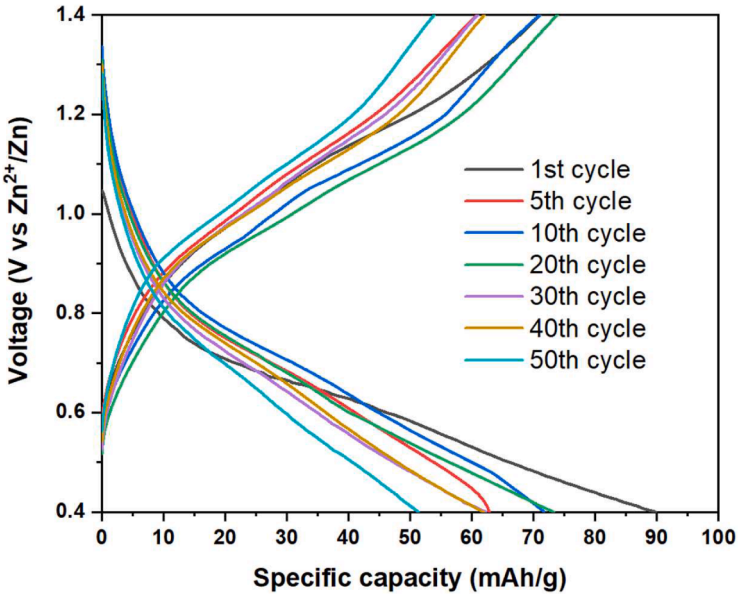

Figure 8. Voltage profiles obtained from a KVO||Zn cell at 10 mA/g for 50 cycles.

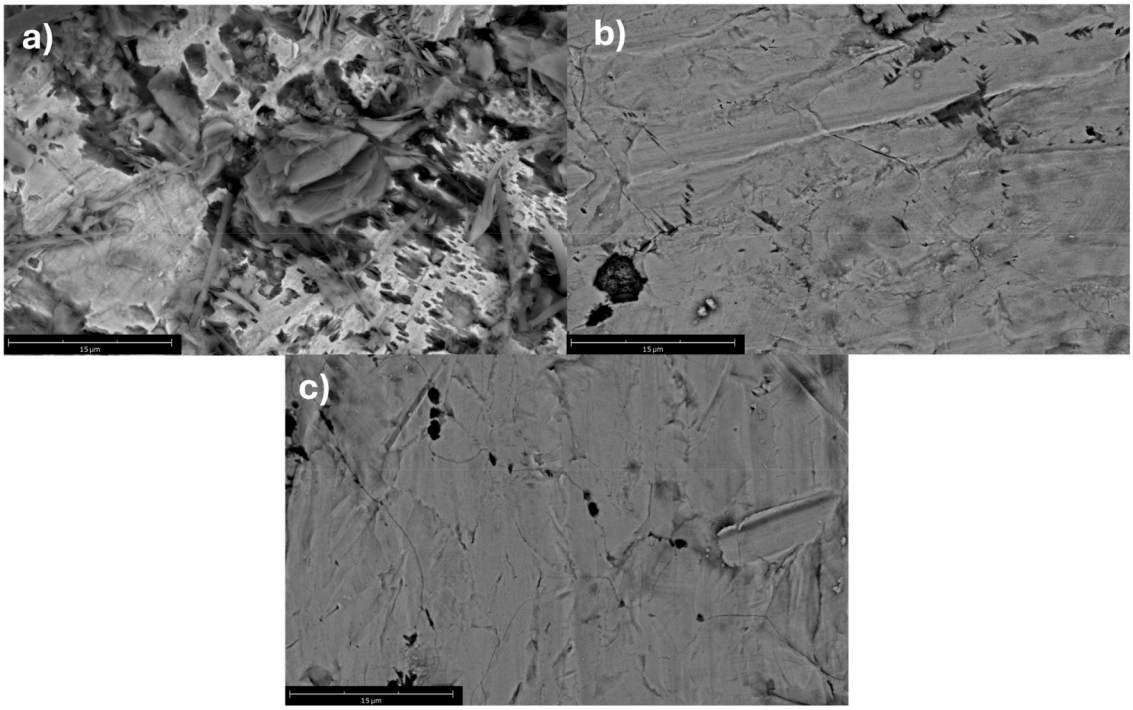

Figure 9. SEM images of electrodes from cells with a) 2 M solution of $ZnSO_4$ electrolyte b) 1:7 Zn/EG electrolyte. c) SEM image of a pristine zinc electrode.

Despite all the challenges, the ethylene glycol:$Zn(TFSI)_2$ LTT mixture appears to be a promising electrolyte system for zinc-ion cells, particularly due its suppression of dendrite growth and cycling stability. A potential approach to overcome the limited capacity due to the high viscosity is the introduction of a co-solvent in the mixture, such as a minimal amount of water. Water has indeed proven to be an appealing additive to deep eutectic solvents to reduce their viscosity[9,11,24,25]. When the amount of water is small enough, activity of water molecules is reduced, possibly inhibiting the usual degradation processes associated with water-based electrolytes for zinc batteries. Additionally, another possible approach recently proposed is the use of a not-coordinating low-viscosity co-solvent, realizing the so-called "locally concentrated deep eutectic electrolytes, LCDEEs"[26], providing at the same time a reduction of viscosity without compromising the solvation sheath of zinc. These approaches will be explored in future works.

4. Conclusions

Low-transition-temperature electrolytes of $Zn(TFSI)_2$ and ethylene glycol were prepared by mixing them in different molar ratios. Thermal analyses demonstrated notable stability at low temperatures for all mixtures, without any phase transitions observed down to -80°C. ATR-FTIR confirmed the presence of interactions between the salt and the solvent, while Raman spectroscopy highlighted that at least 10% of the anions takes part in the solvation structure of the Zn-ions in electrolytes with a Zn:EG molar ratio up to 1:9. Electrochemical tests revealed that the electrolyte with a Zn:EG ratio of 1:7 exhibited the highest reversibility for Zn plating/stripping and a satisfying ionic conductivity at room-temperature. Symmetric Zn cells with this electrolyte sustained continuous plating/stripping for approximately 150 hours and in a full Zn||KVO cell it showed excellent cycling stability up to 50 cycles, enabled by more homogeneous plating of Zn, but a limited specific capacity due to the high viscosity.

CRediT authorship contribution statement

Matteo Palluzzi: Writing – original draft, Visualization, Validation, Investigation, Data curation. **Marita Afiandika:** Validation, Investigation. **Shizhao Xiong:** Writing – review & editing, Supervision, Methodology, Formal analysis. **Akiko Tsurumaki:** Writing – review & editing, Supervision. **Paola D'Angelo:** Writing – review & editing, Supervision. **Aleksandar Matic:** Writing – review & editing, Supervision, Resources, Methodology, Funding acquisition, Conceptualization. **Maria Assunta Navarra:** Writing – review & editing, Supervision, Resources, Project administration, Methodology, Funding acquisition, Conceptualization.

Declaration of competing interest

The authors declare that they have no known competing financial interests or personal relationships that could have appeared to influence the work reported in this paper.

Acknowledgements

AM and MA acknowledge funding from the Knut and Alice Wallenberg Foundation (KAW) through the Wallenberg Wood Science Center. M.P. thanks Sapienza University of Rome for funding Progetto per Avvio alla Ricerca-Tipo 1 (AR123188B4B6E3E0) and the PhD students' mobility abroad. MP also acknowledges the PhD program on green topics of the PON Research and Innovation 2024-2020. M.A.N. thanks the financial support of the National Recovery and Resilience Plan (PNRR), Mission 4 Component 2 Investment 1.3, funded from the European Union Next Generation EU, within the Spoke 6 "Energy Storage" of the Extended Partnership (PE2) NEST - Network 4 Energy Sustainable Transition" (CUP B53C22004070006). The support of Dr. Giovanni Battista Appetecchi and Maria Di Pea (ENEA, Italy) for conductivity measurements is gratefully acknowledged.

Supplementary materials

Supplementary material associated with this article can be found, in the online version, at doi:10.1016/j.electacta.2025.146061.

Data availability

Data will be made available on request.

References

[1] A. Innocenti, D. Bresser, J. Garche, S. Passerini, A critical discussion of the current availability of lithium and zinc for use in batteries, Nat Commun 15 (2024) 4068.
[2] L. Stievano, et al., Emerging calcium batteries, Journal of Power Sources 482 (2021) 228875.
[3] W. Kao-ian, et al., Stability Enhancement of Zinc-Ion Batteries Using Non-Aqueous Electrolytes, Batteries & Supercaps 5 (2022).
[4] H. Li, et al., Electrolyte Strategies Facilitating Anion-Derived Solid-Electrolyte Interphases for Aqueous Zinc–Metal Batteries, Small Methods 2300554 (2023), https://doi.org/10.1002/smtd.202300554.
[5] M. Francisco, A. van den Bruinhorst, M.C. Kroon, Low-Transition-Temperature Mixtures (LTTMs): A New Generation of Designer Solvents, Angew Chem Int Ed 52 (2013) 3074–3085.
[6] L. Geng, et al., Eutectic Electrolyte with Unique Solvation Structure for High-Performance Zinc-Ion Batteries, Angew Chem Int Ed 61 (2022).
[7] H. Qiu, et al., Zinc anode-compatible in-situ solid electrolyte interphase via cation solvation modulation, Nat Commun 10 (2019) 5374.
[8] J. Wang, et al., Eutectic electrolytes with leveling effects achieving high depth-of-discharge of rechargeable zinc batteries, Energy Storage Materials 58 (2023) 9–19.
[9] M. Han, et al., Hydrated Eutectic Electrolyte with Ligand-Oriented Solvation Shell to Boost the Stability of Zinc Battery, Adv Funct Materials 32 (2022) 2110957.
[10] G.M. Thorat, V.-C. Ho, J. Mun, Zn-Based Deep Eutectic Solvent as the Stabilizing Electrolyte for Zn Metal Anode in Rechargeable Aqueous Batteries, Front. Chem. 9 (2022) 825807.
[11] W. Yang, et al., Hydrated Eutectic Electrolytes with Ligand-Oriented Solvation Shells for Long-Cycling Zinc-Organic Batteries, Joule 4 (2020) 1557–1574.
[12] M. Jablonský, J. Šima, Is it correct to name DESs deep eutectic solvents? BioRes 17 (2022) 3880–3882.
[13] F. Cappelluti, et al., Stepping away from serendipity in Deep Eutectic Solvent formation: Prediction from precursors ratio, Journal of Molecular Liquids 367 (2022) 120443.
[14] S. Islam, et al., K^+ intercalated V_2O_5 nanorods with exposed facets as advanced cathodes for high energy and high rate zinc-ion batteries, J. Mater. Chem. A 7 (2019) 20335–20347.
[15] B.D. Adams, J. Zheng, X. Ren, W. Xu, J. Zhang, Accurate Determination of Coulombic Efficiency for Lithium Metal Anodes and Lithium Metal Batteries, Adv. Energy Mater. 8 (2018) 1702097.
[16] P. Kolandaivel, V. Nirmala, Study of proper and improper hydrogen bonding using Bader's atoms in molecules (AIM) theory and NBO analysis, Journal of Molecular Structure 694 (2004) 33–38.
[17] V.V. Kuzmin, et al., Correlations among the Raman spectra and the conformational compositions of ethylene glycol, 1,2- and 1,3-propylene glycols, Journal of Molecular Structure 1243 (2021) 130847.
[18] S.O. Liubimovskii, et al., Raman structural study of ethylene glycol and 1,3-propylene glycol aqueous solutions, Spectrochimica Acta Part A: Molecular and Biomolecular Spectroscopy 285 (2023) 121927.
[19] J. Pitawala, A. Martinelli, P. Johansson, P. Jacobsson, A. Matic, Coordination and interactions in a Li-salt doped ionic liquid, Journal of Non-Crystalline Solids 407 (2015) 318–323.
[20] D. Reuter, C. Binder, P. Lunkenheimer, A. Loidl, Ionic conductivity of deep eutectic solvents: the role of orientational dynamics and glassy freezing, Phys. Chem. Chem. Phys. 21 (2019) 6801–6809.
[21] G.B. Appetecchi, Safer electrolyte components for rechargeable batteries, Physical Sciences Reviews 4 (2019).
[22] Q. Li, A. Chen, D. Wang, Z. Pei, C. Zhi, "Soft Shorts" Hidden in Zinc Metal Anode Research, Joule 6 (2022) 273–279.
[23] Q. Yang, et al., Dendrites in Zn-Based Batteries, Advanced Materials 32 (2020) 2001854.
[24] R. Chen, et al., A hydrated deep eutectic electrolyte with finely-tuned solvation chemistry for high-performance zinc-ion batteries, Energy Environ. Sci. 16 (2023) 2540–2549.
[25] J. Shi, et al., Water-in-Deep Eutectic Solvent" Electrolytes for High-Performance Aqueous Zn-Ion Batteries, Adv. Funct. Mater. 31 (2021) 2102035.
[26] C. Xu, T. Diemant, X. Liu, S. Passerini, Locally Concentrated Deep Eutectic Liquids Electrolytes for Low-Polarization Aluminum Metal Batteries, Advanced Materials 36 (2024) 2400263.